Preliminary Validation of Multimodal Feature Matching Method for Multi-source DEM Registration in Planetary Scenarios

Yi Zhang [1], Genyi Wan [1], Dayong Liu [1], Tao Tao [1], Changjiang Xiao [12], Zhen Ye [12], Xiaohua Tong [12]

[1] College of Surveying and Geoinformatics, Tongji University, Shanghai, China
[2] Shanghai Key Laboratory for Planetary Mapping and Remote Sensing for Deep Space Exploration, Shanghai, China

Keywords: DEM registration, Planetary multi-source DEM, Weighted Structure Saliency Feature, Multi-modal image matching.

Abstract

The registration of multi-source Digital Elevation Models (DEMs) is essential for planetary exploration, as it enhances the spatial and temporal coverage of DEM datasets, enabling a broad range of surveying and mapping applications. However, various factors, including the diversity of terrain representations, the weak texture in planetary environments and minimal topographic relief, undermine the effectiveness of common DEM registration methods, making the alignment of planetary multi-source DEMs still a challenging task. To address the nonlinear expression problem in multi-source DEMs, we compared the matching results of various multi-modal matching methods on DEMs from Mars and moon, and selected the best one to construct a robust coarse-to-fine PMS-DEM registration method. Experiments were conducted using multi-source DEM data on Mars and the Moon to assess the effectiveness of the proposed method. The results of image feature matching experiments demonstrate that the Weighted Structure Saliency Feature (WSSF) method outperforms other existing state-of-the-art multimodal matching methods. Besides, the results of DEM registration experiments demonstrate that the reliability of the proposed method compared with other commonly used registration methods.

1. Introduction

Accurate matching and spatial reference unification of topographic data from diverse sources are essential for the effective integration of planetary multi-source data. Planetary multi-source digital elevation models (PMS-DEM) can offer valuable information in scientific research. However, due to the variations in data sources and DEM generation methods, significant differences in terrain representation and weak texture information are often present across different DEMs. These challenges make the precise registration of PMS-DEM datasets complicate (Wu et al., 2013; Huang et al., 2024a; Huang et al., 2025).

DEM registration typically involves coarse registration stage and fine registration stage. Some of the most widely used fine registration methods, like the Iterative Closest Point (ICP) algorithm, are highly effective (Besl and McKay, 1992), but sensitive to the initial orientation. In complete DEM registration process, the coarse registration step is responsible for generating reliable initial values for the fine registration algorithm, which ensures both the correctness and accuracy of the final results. Coarse alignment methods can be generally classified into 3D element-based approaches and 2D image-based approaches. The former relies on extracting 3D features such as points, terrain slopes, or aspect information (Nuth and Kääb, 2011). However, these methods struggle with DEMs exhibiting minimal terrain relief, since extracting high-quality 3D features in such cases is a difficult task. In contrast, 2D image-based methods excel in such scenarios. Feature-based methods in image-based methods are relatively robust to geometric transformations and could be more feasible in practical DEM registration situations. Multi-modal feature matching methods offer great advantages in image matching, as DEMs from different sources typically have distinct representations in images. In recent years, a number of advanced techniques have been introduced in this field (Li et al., 2019, Yao et al., 2022, Zhang et al., 2023, Wan et al., 2024, Huang et al., 2024b), which provides a new way for the research of DEM registration method. However, since these matching methods are designed for Earth remote sensing images, many of them might face challenges when dealing with PMS-DEM data with high-frequency noise and weak texture information. Among these methods, the Weighted Structure Saliency Feature (WSSF) approach achieves more robust matching results compared to other image matching methods in planetary scenes. Is is due to the use of Pointwise Shape-Adaptive Texture Filtering (PSATF) employed in this method to smooth images while preserving structural features (Wan et al., 2024). This design allows WSSF to effectively mitigate the impact of noise and weak texture information in PMS-DEMs.

In this study, we employed the WSSF method to obtain image matching results for PMS-DEM data of various terrains on Mars and the Moon, and compare them with a baseline method. On the basis of WSSF, a robust coarse-to-fine PMS-DEM registration method is proposed, which combines the advantages of feature-based coarse registration methods and ICP-based fine registration methods. First, the PMS-DEM data are preprocessed to facilitate the subsequent steps. Then, feature matching method WSSF is utilized to obtain matching results for the preprocessed PMS-DEM images. Subsequently, 3D feature point pairs are constructed to facilitate the coarse registration of PMS-DEMs. After that, PMS-DEMs are sampled into discrete point clouds, and the ICP algorithm is applied to refine the results in fine registration stage. Finally, the rasterisation of the transformed point clouds generate the accurately aligned DEM outputs.

2. Methodology

Fig. 1 shows the proposed coarse-to-fine PMS-DEM alignment framework, including data pre-processing, coarse registration, and fine registration.

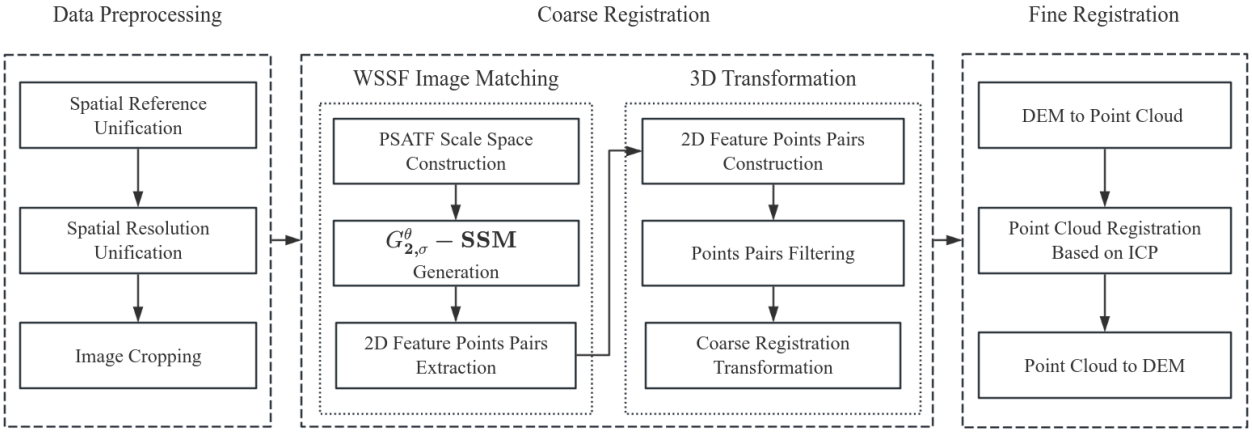

Figure 1. The workflow of proposed DEM registration method

2.1 Data Preprocessing

In experiments, DEMs would be rasterized and elevation information would be encoded into image grayscale. Before performing the PMS-DEM registration process, it is necessary to preprocess DEM data from different sources.

First of all, the spatial reference frameworks of the source DEM and reference DEM must be unified. Through re-projection process, the spatial projection coordinate system of the source DEM data could be adjusted to align with the projection coordinate system of the reference DEM.

Subsequently, it is necessary to unify the spatial resolution of the source DEM and the reference DEM, and change the resolution of the source DEM data to be consistent with the reference DEM through resampling.

On this basis, the source DEM and reference DEM with unified spatial coordinate system and spatial resolution are cropped into rectangles of the same size for subsequent PMS-DEM registration.

2.2 Image Matching Between PMS-DEM Image

In this section, the WSSF method is used to achieve 2D feature point matching results on PMS-DEM images.

First, the PSATF is used in constructing the scale space, enabling image smoothing while preserving structural features. The concept of PSATF is defined as follows:

$$J_p = \frac{\sum_{q \epsilon N(p)} G_{\sigma_s}(p,q) \cdot M_{\sigma_r}(I_p, I_q) \cdot I_q}{\sum_{q \epsilon N(p)} G_{\sigma_s}(p,q) \cdot M_{\sigma_r}(I_p, I_q)}$$

where $G_{\sigma_s}(p,q) \cdot M_{\sigma_r}(I_p, I_q)$ represents the weight of pixel q to the output of pixel p, with $G_{\sigma_s}(p,q)$ denotes the Gaussian filtering of scale σ_s and $M_{\sigma_r}(I_p, I_q)$ represents a filtering that guides the image; J_p and I_q are the pixel values of the image output and input respectively; p and q denote the index positions of pixels in the image, while scale σ_s and σ_r are set to 0.05 (Wan et al., 2024). Compared to other filter such as co-occurrence filter (Jevnisek and Avidan, 2017) and Relative Total Variation (RTV) filter (Xu et al., 2012), PSATF highlights similar structural information in PMS-DEM data with different expressions while image smoothing, improving the robustness of multi-modal image matching.

Next, the structural saliency map combined with the second-order Gaussian steerable filtering ($G^{\theta}_{2,\sigma} - \mathrm{SSM}$) is generated based on phase features, second-order Gaussian steerable filtering ($G^{\theta}_{2,\sigma}$), and Edge Confidence Map (ECM) . $G^{\theta}_{2,\sigma} - \mathrm{SSM}$ enhances local spatial information while collecting overall structural information of images, which can better capture significant features of multi-modal images (Wan et al., 2024).

The FAST (Rosten and Drummond, 2006) detector is then utilized to identify keypoints on $G^{\theta}_{2,\sigma} - \mathrm{SSM}$, which are subsequently described through the improved GLOH descriptor (Mikolajczyk and Schmid, 2005). Then the described keypoints are utilized for initial matching. At the end of image matching, the Fast Sample Consistency (FSC) method (Wu et al., 2015) is used to screen connection points that meet the threshold conditions and obtain the final matching result.

2.3 Coarse-to-Fine DEM Registration

DEM image matching enables horizontal registration between the source DEM and the reference DEM. Traditional 2D image-based DEM registration methods sometimes first perform horizontal alignment, followed by the correction of elevation differences to remove vertical offset. However, these methods cannot address 3D rotation (tilt) between PMS-DEMs. To eliminate the tilt between the PMS-DEM data, a 3D similarity transformation matrix is computed using corresponding points from both DEMs.

The construction of 3D feature point pairs is an important prerequisite for the calculation of 3D transformation matrix. At the beginning, the pixel coordinates of the corresponding points on the DEM image need to be converted into DEM's spatial coordinate system. Using the spatial information of the DEM (coordinate system, spatial resolution, etc.) and the previous matching results, the spatial coordinates of the corresponding points on the source and reference DEMs can be restored. Then, the elevation values of the PMS-DEM at the matching locations are extracted and combined with the horizontal coordinates to construct 3D feature point pairs.

Subsequently, the 3D similarity transformation matrix for coarse registration can be calculated based on 3D feature point pairs. A

similarity transformation model is chosen for the PMS-DEM coarse registration, consisting of a rotation matrix $R_{3\times3}$ and a translation vector $T_{3\times1}$, which are determined through the Singular Value Decomposition (SVD) method (Eggert et al., 1997). At last, the calculated 3D similarity transformation matrix is applied to the source DEM, accomplishing the coarse registration of the PMS-DEM.

A good initial position for the subsequent fine registration is provided by the previous coarse registration step. At the beginning of the fine registration step, the coarsely aligned PMS-DEMs are first sampled as two discrete point clouds. After that, the ICP algorithm is applied to the discrete point cloud data in order to further reduce the deviation between source point cloud and target point cloud. Finally, the transformed source point cloud data is rasterized to generate the PMS-DEM after fine registration.

3. Experimental Details

3.1 Experimental Data

Experiments were carried out using PMS-DEMs of the Mars and the Moon to assess the effectiveness of the proposed method.

The PMS-DEM data for Mars consisted of optical DEMs derived from two distinct optical stereo image pairs, including data from the High Resolution Imaging Science Experiment (HiRISE) and the Context Camera (CTX). The CTX DEMs were generated in-house through photogrammetric processing of CTX stereo image pairs, while the HiRISE DEMs were obtained from publicly available datasets.

Unlike the experimental data on Mars consist of optical DEMs from different sensors, the lunar experiment tested the registration between optical DEM and laser-based DEM. The laser-based DEM used in the experiment is the SLDEM, derived from the Lunar Orbiter Laser Altimeter (LOLA) data. The optical DEM used in the study was generated from the CCD images of the Chang'e-2 (CE-2) mission.

Planetary	Type	Source	Resolution	Number
Mars	HiRISE DEM / CTX DEM	NASA-1 / Self-products	1m / 10m	6
Moon	CE-2 DEM / SLDEM	GRAS / NASA-2	20m / 60m	6

Table 1. Basic information about the used PMS-DEMs

3.2 Experimental Settings

In this experiment, the proposed coarse-to-fine PMS-DEM registration method are compared with other commonly used DEM registration methods, such as pc_align tool in the Ames Stereo Pipeline (ASP) (Beyer et al., 2011).

The ICP refinement step is included in all DEM registration methods. At this stage, the performance is evaluated using the Mean Absolute Error (MAE), which is calculated as:

$$MAE_{DEM} = \frac{1}{N}\sum_{i=1}^{N}\left|h_{src,i} - h_{ref,i}\right|$$

where $h_{src,i}$ and $h_{ref,i}$ are the elevation value of the source DEM and reference DEM at the i-th position respectively, and N is the pixel number of the specified region. MAE represents the average absolute difference between source DEM height values and reference DEM height values. Compared to Mean Squared Error or Root Mean Squared Error, MAE is less sensitive to outliers because it does not square the errors, which avoids amplifying large differences.

4. Results and Discussion

4.1 Results of PMS-DEM Image Matching

Fig. 2 lists the exemplar DEM image matching results of WSSF on Martian and lunar PMS-DEM experimental datasets, comparing with RIFT (Li et al., 2019) as baseline method.

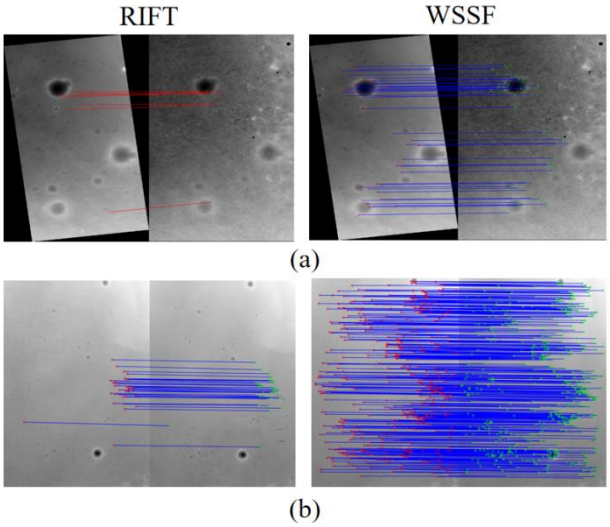

Figure 2. The results of different image matching methods (RIFT and WSSF) on the exemplar images of two PMS-DEM datasets: (a) Results for Martian PMS-DEM; (b) Results for Lunar PMS-DEM.

The method is evaluated based on two aspects: Success Rate (SR) and Number of Correct Matching (NCM). In terms of SR, WSSF achieved correct PMS-DEM image matching across all experimental data for both Martian and lunar PMS-DEM. In contrast, RIFT achieved only a 16.67% success rate in the Mars PMS-DEM experiments, hindered by weak textures and high-frequency noise, while achieving 83.33% in the lunar DEM. As for NCM, WSSF outperformed RIFT across all experimental data, achieving an NCM approximately 5 times higher on Mars and 9 times higher on the Moon. These experimental results indicate that the WSSF method outperforms RIFT in generalization ability and matching accuracy.

4.2 Results of PMS-DEM Registration Experiment

Table 2 presents the registration results of Martian and lunar PMS-DEM data obtained using different DEM registration methods, with partial example cases shown in Fig. 3 and Fig. 4.

	Dataset	Origin	Proposed	ASP
MAD /m	Mars	11.228	2.938	3.155
	Moon	18.055	5.494	7.249

Table 2. Registration results of Martian and Lunar PMS-DEMs

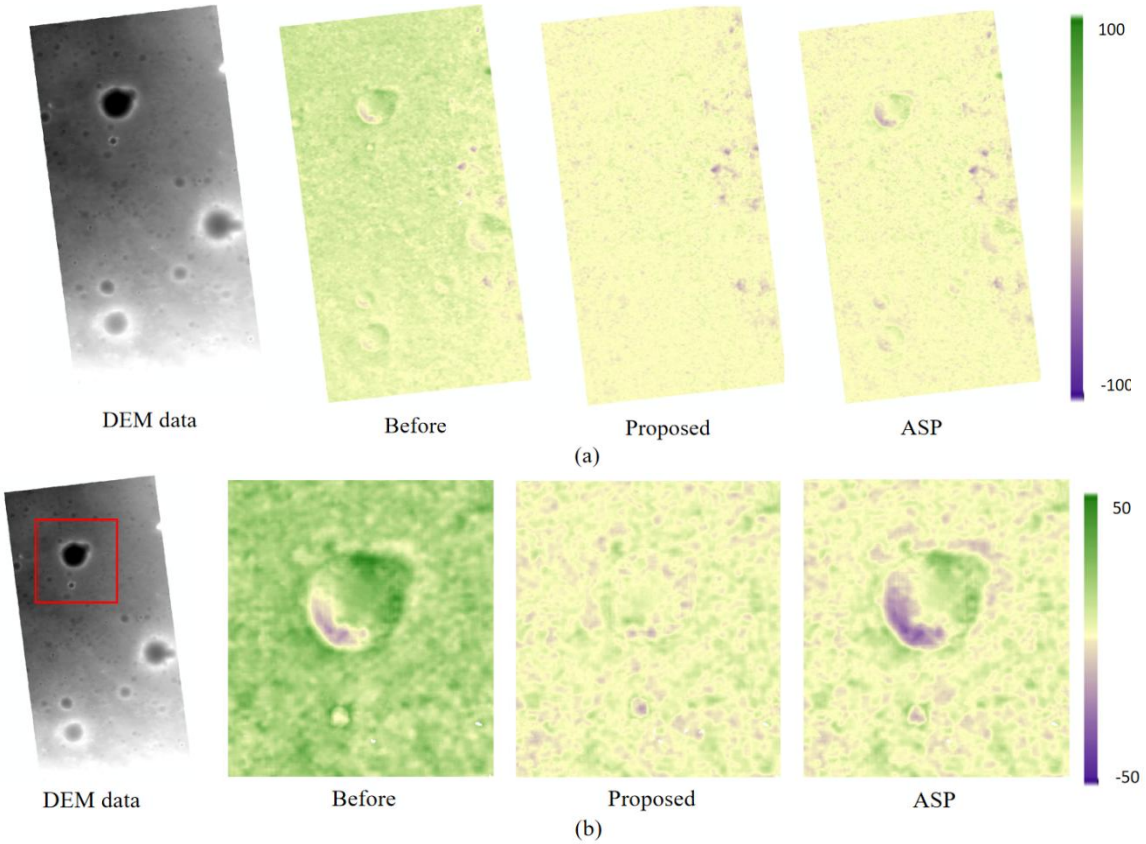

Figure 3. The elevation differences after using different DEM registration methods on the exemplar DEM of Martian PMS-DEM: (a) Full PMS-DEM; (b) Local PMS-DEM.

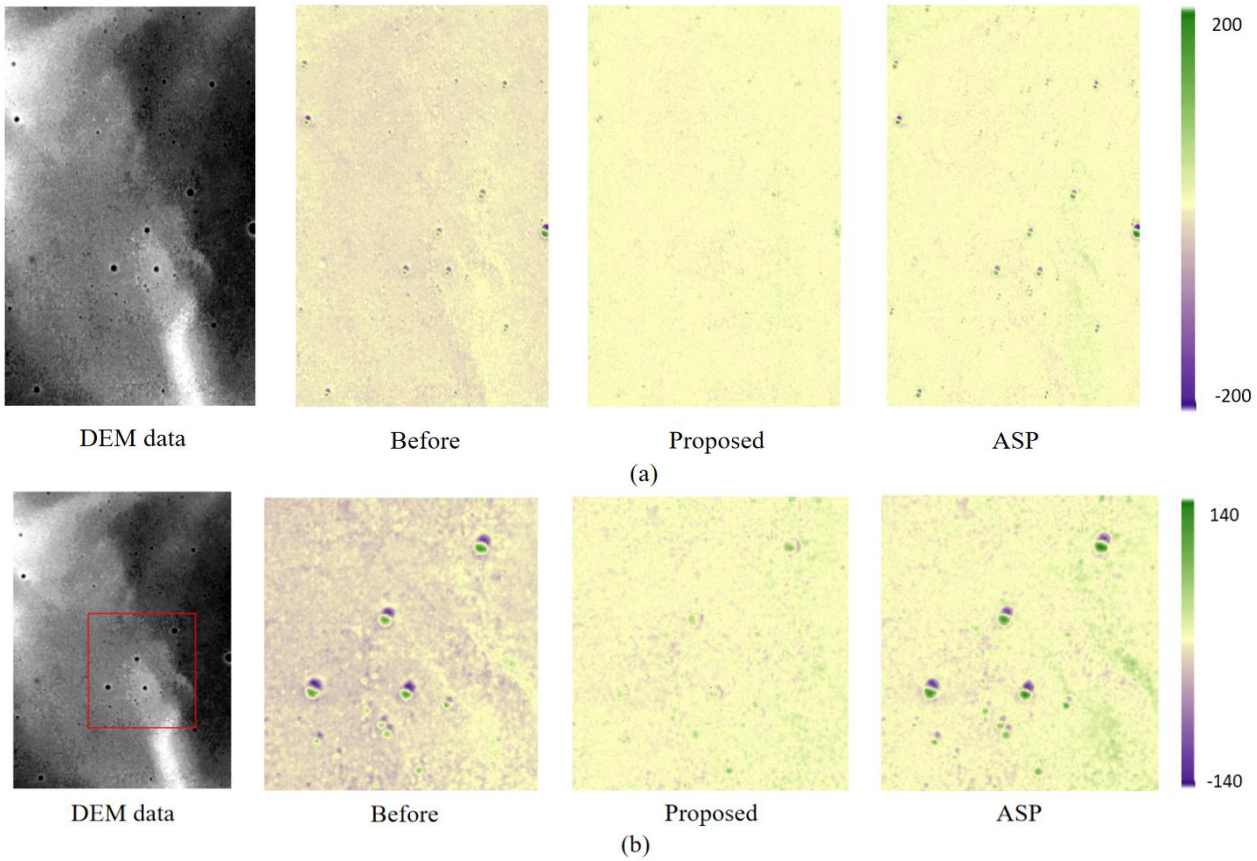

Figure 4. The elevation differences after using different DEM registration methods on the exemplar DEM of Lunar PMS-DEM: (a) Full PMS-DEM; (b) Local PMS-DEM.

https://doi.org/10.5194/isprs-archives-XLVIII-G-2025-1727-2025 | © Author(s) 2025. CC BY 4.0 License.

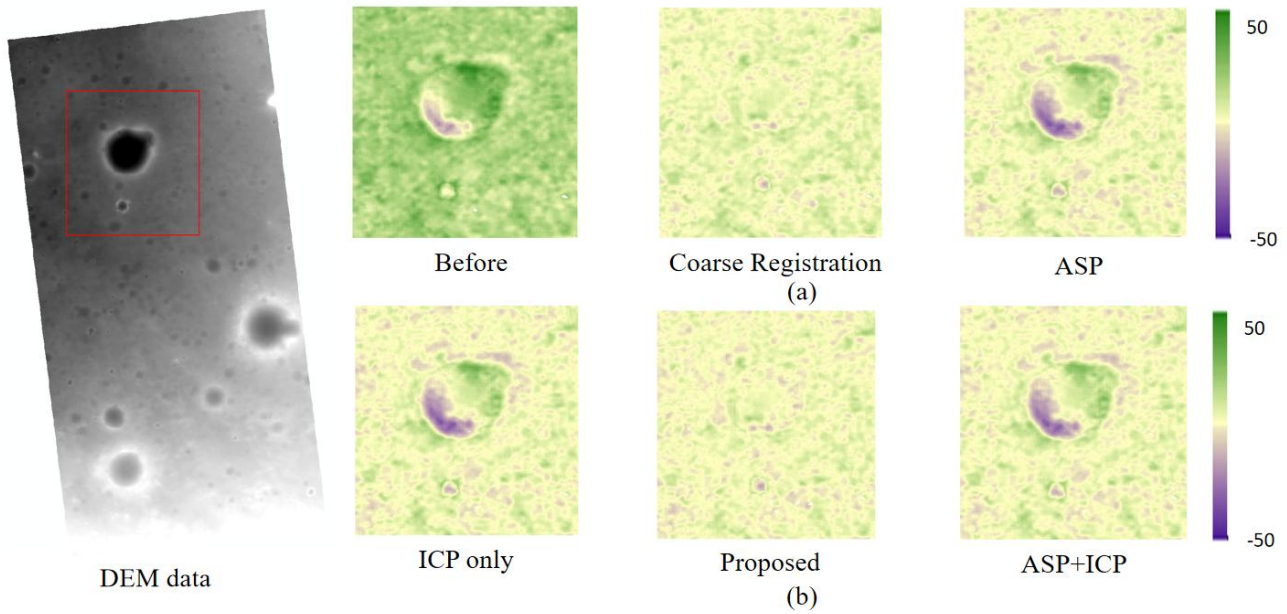

Figure 5. The local elevation differences before and after using ICP algorithm on the exemplar Martian PMS-DEM registered using different methods: (a) Before using ICP; (b) After using ICP.

As shown in Table 2, all methods are capable of reducing the elevation difference between PMS-DEMs, and the proposed registration method achieving the most accurate results. It is because WSSF-based coarse registration provides excellent initial position for ICP processing in fine registration, resulting in high registration accuracy for the overall DEM registration results.

The effectiveness of ASP DEM registration method has been validated in previous studies and widely applied. In PMS-DEM registration experiments on Mars and the Moon, ASP method effectively improved the initial PMS-DEM; however, its limitation was also revealed. For most of the obtained PMS-DEM experimental data, the terrain relief were relatively small and lacked distinct topographic features. Consequently, many DEM registration methods based on terrain characteristics or 3D feature extraction are constrained, while image-based DEM registration methods show significant advantages in such scenarios.

As for the pc_align tool in ASP, we used its default Point-to-Plane ICP method because it is more robust than other ICP methods when dealing with large translations. However, when there is a significant offset between PMS-DEM datasets, the results obtained by ASP may easily fall into a local optimum.

4.3 ICP in PMS-DEM Registration

In this experiment, the ICP algorithm is added to all DEM registration methods to test the effectiveness of the ICP algorithm in refining registration results of each method.

Through the results in Fig. 5, it shows that the ICP algorithm improves the accuracy of all DEM registration methods (Coarse Registration in Fig. 5 (a) corresponds to the WSSF-based coarse registration result of the proposed method). It also shows that for PMS-DEMs with incorrect horizontal alignment, the deviation between PMS-DEM has not been completely eliminated after ICP process.

The experimental results confirm that the ICP algorithm for fine registration has high requirements for coarse registration results. If the initial position is not appropriate, the ICP algorithm may fall into local optimal results and fail to find the global optimal position. This highlights the need for a reliable and accurate coarse registration method, and the WSSF-based coarse registration employed in this study effectively meets this requirement.

5. Conclusion

In this study, we demonstrate the superiority of the WSSF method for PMS-DEM image matching. Besides, we propose a robust coarse-to-fine PMS-DEM registration method using feature matching method. First, WSSF method is used to extract feature points in prepossesed PMS-DEM images to construct 3D correspondence for coarse registration, and then ICP algorithm is applied to further refine the alignment results. The experimental results of PMS-DEM on Mars and Moon show that better results can be achieved by the proposed method compared to other comparative methods, which preliminarily verifies the feasibility of the feature descriptor-based matching method for PMS-DEM registration.

However, for PMS-DEM data with weaker texture information, the image matching achieved using WSSF method did not completely eliminate the horizontal offset between the data. Future work will explore more effective structure extraction methods to further improve the generality and robustness of DEM registration method.

Acknowledgements

The work described in this paper was supported by the National Key R&D Program of China (2022YFF0504100), and in part by the National Natural Science Foundation of China (grant nos. 42221002).

References

Besl, P.J., McKay, N.D., 1992: Method for registration of 3-D shapes. In *Sensor fusion IV: control paradigms and data structures*, 1611, 586-606. doi.org/10.1117/12.57955.

Beyer, R.A., Alexandrov, O., McMichael, S., 2018: The Ames Stereo Pipeline: NASA's open source software for deriving and processing terrain data. *Earth and Space Science*, 5(9), 537-548. doi.org/10.1029/2018EA000409.

Eggert, D., Lorusso A., Fisher R., 1997: Estimating 3-D rigid body transformations: a comparison of four major algorithms. *Machine Vision and Applications*, 9(5), 272-290. doi.org/10.1007/s001380050048.

Huang, R., Chen, C., Wan, G., Xie, H., Xie, J., Feng, J., Xiao H., Tong, X., 2024: A Novel Graph Guided Global Bundle Block Adjustment of OSIRIS-REx Laser Altimeter Data for Topographic Mapping of Asteroid Bennu. *IEEE Transactions on Geoscience and Remote Sensing*, 62, 1-14.

Huang, R., Wan, G., Zhou, Y., Ye, Z., Xie, H., Xu, Y., Tong, X., 2024: Fast Double-channel Aggregated Feature Transform for Matching Planetary Remote Sensing Images. *IEEE Journal of Selected Topics in Applied Earth Observations and Remote Sensing*. doi.org/10.1109/JSTARS.2024.3390432.

Huang, R., Ding, W., Xu, Y., Ye, Z., Xu, S., Zhou, M., Tong, X., 2025: Fusion of multiple photogrammetric DEMs for large-scale lunar topographic mapping. *Advances in Space Research*.

Li, J., Hu, Q., Ai, M., 2019: RIFT: Multi-modal image matching based on radiation-variation insensitive feature transform. *IEEE Transactions on Image Processing*, 29, 3296-3310. doi.org/10.1109/TIP.2019.2959244.

Mikolajczyk, K., Schmid, C., 2005: A performance evaluation of local descriptors. *IEEE Transactions on Pattern Analysis and Machine Intelligence*, 27(10), 1615-1630. doi.org/10.1109/TPAMI.2005.188.

Nuth, C., Kääb, A., 2011: Co-registration and bias corrections of satellite elevation data sets for quantifying glacier thickness change. *The Cryosphere*, 5(1), 271-290. doi.org/10.5194/tc-5-271-2011.

Rosten, E., Drummond, T., 2006: Machine learning for high-speed cornerdetection. In *Computer Vision–ECCV 2006: 9th European Conference on Computer Vision, Graz, Austria, May 7-13, 2006, Proceedings, Part I 9*, 430-443. doi.org/10.1007/11744.

Wan, G., Ye, Z., Xu, Y., Huang, R., Zhou, Y., Xie, H., Tong, X., 2024: Multi-Modal Remote Sensing Image Matching Based on Weighted Structure Saliency Feature. *IEEE Transactions on Geoscience and Remote Sensing*, 62, 1-16. doi.org/ 10.1109/TGRS.2023.3347259.

Wu, B., Guo, J., Hu, H., Li, Z., Chen, Y., 2013: Co-registration of lunar topographic models derived from Chang ’ E-1, SELENE, and LRO laser altimeter data based on a novel surface matchingmethod. *Earth and Planetary Science Letters*, 364, 68-84. doi.org/10.1016/j.epsl.2012.12.024.

Wu, Y., Ma, W., Gong, M., Su, L., Jiao, L., 2015: A novel point-matching algorithm based on fast sample consensus for image registration. *IEEE Geoscience and Remote Sensing Letters*, 12(1), 43 – 47. doi.org/10.1109/LGRS.2014.2325970.

Jevnisek, R.J., Avidan, S., 2017: Co-occurrence filter. In *Proceedings of the IEEE Conference on Computer Vision and Pattern Recognition*, 3184-3192.

Xu, L., Yan, Q., Xia, Y., Jia, J., 2012: Structure extraction from texture via relative total variation. *ACM transactions on graphics (TOG)*, 31(6), 1-10. doi.org/10.1145/2366145.2366158.

Yao, Y., Zhang, Y., Wan, Y., Liu, X., Yan, X., Li, J., 2022: Multi-modal remote sensing image matching considering co-occurrence filter. *IEEE Transactions on Image Processing*, 31, 2584-2597. doi.org/10.1109/TIP.2022.3157450.

Zhang, Y., Yao, Y., Wan, Y., Liu, W., Yang, W., Zheng, Z., Xiao, R., 2023: Histogram of the orientation of the weighted phase descriptor for multi-modal remote sensing image matching. *ISPRS Journal of Photogrammetry and Remote Sensing*, 196, 1-15. doi.org/10.1016/j.isprsjprs.2022.12.018.